

Characteristics of complex network of heatwaves over China

Xuemin Shen(沈雪敏), Xiaodong Hu(胡晓东), Aixia Feng(冯爱霞), Qiguang Wang(王启光), and Changgui Gu(顾长贵)

Citation: Chin. Phys. B, 2025, 34 (**3**): 038903. DOI: 10.1088/1674-1056/ada43a
Journal homepage: http://cpb.iphy.ac.cn; http://iopscience.iop.org/cpb

What follows is a list of articles you may be interested in

Node ranking based on graph curvature and PageRank

Hongbo Qu(曲鸿博), Yu-Rong Song(宋玉蓉), Ruqi Li(李汝琦), Min Li(李敏), and Guo-Ping Jiang(蒋国平)
Chin. Phys. B, 2025, 34 (**2**): 028901. DOI: 10.1088/1674-1056/ad9a9b

Detecting the core of a network by the centralities of the nodes

Peijie Ma(马佩杰), Xuezao Ren(任学藻), Junfang Zhu(朱军芳), and Yanqun Jiang(蒋艳群)
Chin. Phys. B, 2024, 33 (**8**): 088903. DOI: 10.1088/1674-1056/ad4cd4

Identifying influential spreaders in complex networks based on density entropy and community structure

Zhan Su(苏湛), Lei Chen(陈磊), Jun Ai(艾均), Yu-Yu Zheng(郑雨语), and Na Bie(别娜)
Chin. Phys. B, 2024, 33 (**5**): 058901. DOI: 10.1088/1674-1056/ad20d6

A multilayer network diffusion-based model for reviewer recommendation

Yiwei Huang(黄羿炜), Shuqi Xu(徐舒琪), Shimin Cai(蔡世民), and Linyuan Lü(吕琳媛)
Chin. Phys. B, 2024, 33 (**3**): 038901. DOI: 10.1088/1674-1056/ad181d

Source localization in signed networks with effective distance

Zhi-Wei Ma(马志伟), Lei Sun(孙蕾), Zhi-Guo Ding(丁智国), Yi-Zhen Huang(黄宜真), and Zhao-Long Hu(胡兆龙)
Chin. Phys. B, 2024, 33 (**2**): 028902. DOI: 10.1088/1674-1056/ad1482

Characteristics of complex network of heatwaves over China

Xuemin Shen(沈雪敏)[1], Xiaodong Hu(胡晓东)[2], Aixia Feng(冯爱霞)[3], Qiguang Wang(王启光)[4,†], and Changgui Gu(顾长贵)[1]

[1] *School of Business, University of Shanghai for Science and Technology, Shanghai* 200093, *China*
[2] *College of Engineering, China Agricultural University, Beijing* 100083, *China*
[3] *National Meteorological Information Center, Beijing* 100081, *China*
[4] *China Meteorological Administration Training Center, Beijing* 100081, *China*

(Received 5 November 2024; revised manuscript received 23 December 2024; accepted manuscript online 31 December 2024)

Using complex network methods, we construct undirected and directed heatwave networks to systematically analyze heatwave events over China from 1961 to 2023, exploring their spatiotemporal evolution patterns in different regions. The findings reveal a significant increase in heatwaves since the 2000s, with the average occurrence rising from approximately 3 to 5 times, and their duration increasing from 15 to around 30 days, nearly doubling. An increasing trend of "early onset and late withdrawal" of heatwaves has become more pronounced each year. In particular, eastern regions experience heatwaves that typically start earlier and tend to persist into September, exhibiting greater interannual variability compared to western areas. The middle and lower reaches of the Yangtze River and Xinjiang are identified as high-frequency heatwave areas. Complex network analysis reveals the dynamics of heatwave propagation, with degree centrality and synchronization distance indicating that the middle and lower reaches of the Yangtze River, Northeast China, and Xinjiang are key nodes in heatwave spread. Additionally, network divergence analysis shows that Xinjiang acts as a "source" area for heatwaves, exporting heat to surrounding regions, while the central region functions as a major "sink," receiving more heatwave events. Further analysis from 1994 to 2023 indicates that heatwave events exhibit stronger network centrality and more complex synchronization patterns. These results suggest that complex networks provide a refined framework for depicting the spatiotemporal dynamics of heatwave propagation, offering new avenues for studying their occurrence and development patterns.

Keywords: complex network, heatwave, spatiotemporal evolution characteristics

PACS: 89.75.Fb, 92.70.Mn, 92.70.Kb

DOI: 10.1088/1674-1056/ada43a **CSTR:** 32038.14.CPB.ada43a

1. Introduction

The Sixth Assessment Report on Climate Change highlights a clear trend of global warming over the past decade (2011–2020), characterized by a rapid increase in the intensity and frequency of extreme weather and climate events. This has resulted in widespread impacts and serious disasters.[1,2] Among all countries, China stands out as a particularly sensitive area affected by global climate change, with many regions experiencing a rate of temperature rise significantly higher than the global average during the same period.[3,4] Consequently, high temperatures and the associated heatwaves have markedly increased across various parts of China, drawing considerable attention from researchers.[5–11] In recent years, studies focusing on the spatial and temporal variability of heatwaves, as well as their associated risks, have proliferated, often employing linear mathematical and statistical methods to analyze their changing characteristics.[12] From 1951 to 2020, the average annual surface temperature in China rose significantly by 0.26 °C per decade, while the average number of extreme high-temperature days increased by approximately 8.5%. Regions in the east and northwest are projected to face even more intense extreme heat.[2,13] Overall, there has been a substantial rise in the number of extreme high-temperature days throughout much of China, although this distribution reveals significant regional disparities.[14–17]

However, as heatwaves become more frequent and intense, their evolutionary processes often grow more complex, with nonlinear characteristics increasingly prominent.[18] Traditional statistical methods, while capable of revealing the spatiotemporal distribution of heatwaves, have notable limitations in capturing their intricate propagation pathways, interregional associations, and evolutionary patterns. A clear understanding of these spatial characteristics is crucial for improving the predictability of extreme weather events and formulating effective high-risk prevention measures.[19,20] Consequently, there is an urgent need for multi-perspective and in-depth analyses of heatwaves. The rise of complex networks provides new methodologies and possibilities for uncovering these intricate dynamic processes.

In recent years, the application of complex network theory to extract valuable information from time series has emerged as a prominent research frontier across various

†Corresponding author. E-mail: wangqg@cma.gov.cn

© 2025 Chinese Physical Society and IOP Publishing Ltd. All rights, including for text and data mining, AI training, and similar technologies, are reserved.

disciplines,[21–23] such as financial markets, social networks, and disease transmission.[24,25] In the field of meteorology, there are also numerous studies utilizing complex network methods to explore the intricate structures of climate system.[26–35] Zhou *et al.*[36] applied a coarse-graining method to process China's temperature series and constructed a temperature fluctuation network. They also built random and chaotic fluctuation networks based on random sequences and chaotic sequences from the Lorenz system, respectively, to compare the intrinsic properties of these three types of sequences from a network perspective. Yang *et al.*[37] investigated the influence of seasonal factors on climate networks and found that the overall characteristic parameters of the climate network remained relatively stable across different seasons. However, the community structure and local node topological connections of the network exhibited significant seasonal variations. Compared to traditional approaches, complex networks offer distinct advantages in understanding the complex evolution and coupling of extreme climate events. They can capture topological information such as degree distribution, network diameter, and clustering coefficient, that conventional methods overlook.[38] The application of complex networks in China's meteorology currently focuses primarily on single elements such as temperature and precipitation, while network analysis specifically targeting heatwave events remains relatively limited and in its early stages. Consequently, after applying traditional statistical methods to identify the temporal evolution trends and spatial distribution characteristics of heatwaves in China from 1961 to 2023, this study established both undirected networks representing the synchronization characteristics of heatwaves and directed networks indicating their propagation directions through event synchronization methods. By analyzing network coefficients, the research explored the dynamic connections, spatial propagation, and topological structures of heatwaves across different regions in China. This approach highlights the relationship between network topological features and heatwaves, providing a comprehensive framework for analyzing their spatiotemporal characteristics and offering new perspectives and methodologies for studying their variations, thereby supporting scientific decision-making.

2. Data and methods

2.1. Data

The data used in this study is the $0.5^\circ \times 0.5^\circ$ daily surface temperature dataset for China, which is based on the latest compilation of fundamental data from 2472 National Surface Meteorological Stations. Utilizing the Thin Plate Spline method combined with three-dimensional (3D) geographic spatial information for spatial interpolation, this dataset provides daily temperature grid data with a resolution of $0.5^\circ \times 0.5^\circ$ since January 1961. The study focuses on daily maximum temperatures, with the research period spanning from May to October each year from 1961 to 2023, covering a total of 3830 grid points.

2.2. Methods

2.2.1. Definition and metrics of heatwaves

Currently, there is no universally accepted standard for defining heatwaves.[39,40] Different studies propose various definitions; however, it is generally agreed that heatwaves represent periods of sustained elevated temperatures.[41] This study adopts the widely used relative threshold method for defining heatwaves, identifying a heatwave at a given grid point as a period of three or more consecutive days with daily maximum temperatures at or above the 90th percentile of the temperature series.[42,43]

Based on this definition, relevant statistical metrics are constructed, including heatwave frequency, total heatwave days, earliest onset date, and latest end date. For each grid point, heatwave frequency is defined as the total number of events during the study period, which helps identify regions with frequent and high occurrences over China. Heatwave duration is categorized into total duration, average duration, and maximum duration, representing, respectively: the cumulative number of heatwave days over the 63-year period, the average duration of individual event, and the longest duration of a single event within the period. These metrics highlight areas with higher intensity and more extreme events. Additionally, the frequency distribution of the earliest onset and latest end dates each year provides a clear indication of whether heatwaves tend to occur earlier or persist later over time.

After identifying all heatwave events at each grid point from May to October over the entire study period, the days with heatwave occurrence are marked as '1', while the days without heatwave occurrence are marked as '0'. In this way, for each grid point, the time series of daily maximum temperatures is transformed into a binary time series representing the presence or absence of heatwave events.

2.2.2. The event synchronization theory and complex network

The concept of event synchronization (ES) has previously been applied in climate-extreme related researches, such as extreme precipitation events, drought propagation, and streamflow analysis.[44] For any two grid locations i and j, ES measures the magnitude of synchronization by counting the number of temporally coinciding heatwaves after allowing a possibility of dynamic delay between them.

Let us assume that an event occurs at time t_l^i at grid point i and t_m^j at grid point j ($l = 1, 2, \ldots, s_i$, $m = 1, 2, \ldots, s_j$) within

a variable time lag τ_{lm}^{ij}. This variable time lag is defined as follows:

$$\tau_{lm}^{ij} = \min\left\{\frac{t_{l+1}^{i}-t_{l}^{i}, t_{l}^{i}-t_{l-1}^{i}, t_{m+1}^{j}-t_{m}^{j}, t_{m}^{j}-t_{m-1}^{j}}{2}\right\}, \quad (1)$$

where s_i and s_j are the total number of such events at locations i and j respectively. Now we define $c(i|j)$ and $c(j|i)$ as the number of times an event appear at location i after it appears at location j and *vice versa*, respectively. The definition of $c(i|j)$ is as follows:

$$c(i|j) = \sum_{l=1}^{s_i}\sum_{m=1}^{s_j} J_{ij}, \quad (2)$$

where

$$J_{ij} = \begin{cases} 1, & \text{if } 0 < t_l^i - t_m^j < \tau_{lm}^{ij}, \\ 0.5, & \text{if } t_l^i = t_m^j, \\ 0, & \text{if otherwise.} \end{cases} \quad (3)$$

Similarly, we can define $c(j|i)$. Now we define

$$Q_{ij} = \frac{c(i|j)+c(j|i)}{\sqrt{s_i s_j}}, \quad (4)$$

$$q_{ij} = \frac{c(i|j)-c(j|i)}{\sqrt{s_i s_j}}, \quad (5)$$

where Q_{ij} is a measure of the strength of synchronization of heatwaves between grid points i and j whereas q_{ij} measures the delay between them. Following Eqs. (4) and (5), $Q_{ij} = 1$ indicates complete synchronization between the heatwaves of i and j whereas $q_{ij} = 1$ means that events at grid point i always precede events at grid point j.

In the current study, ES has been implemented with a maximum possible time delay of 3 days, thus we set $\tau_{\max} = 3$. This means that two events will only be considered synchronous if the temporal gap between their occurrences does not exceed 3 days. Upon completion of the ES computation, we can obtain synchronization and delay matrices, each with dimensions of 3830×3830.

Two different complex networks, undirected and directed complex networks, from the synchronization and delay matrix have been constructed with the assumption that every grid point act as a vertex of the network while the connections between them are the edges.

The synchronization matrix is utilized to develop the undirected complex network with the assumption that two points are connected only if the synchronization between them belongs to the strongest 5% of all the synchronization values. Similarly, directed network is constructed from the delay matrix with the threshold for a connection being the 95th percentile value in magnitude of all the delay values. The methods for converting both the synchronization matrix and the delay matrix to binary adjacency matrices are as follows:

$$A_{ij}^{Q} = \begin{cases} 1, & \text{if } Q_{ij} > \theta, \\ 0, & \text{if otherwise,} \end{cases} \quad (6)$$

$$A_{ij}^{q} = \begin{cases} 1, & \text{if } q_{ij} > |\delta|, \\ 0, & \text{if otherwise,} \end{cases} \quad (7)$$

where θ and δ represent the thresholds for undirected and directed connections respectively. Now we have two complex networks $\boldsymbol{A}^{Q}$ and $\boldsymbol{A}^{q}$ with the first giving us the magnitude of synchronization and the second one providing us with a direction of propagation of heatwaves.

From the undirected network, we derive three network coefficients, namely degree centrality (DC), synchronized distance (SD), and clustering coefficient (CC). And we derive network divergence (ND) from the directed network. The formulas for calculating these coefficients are as follows:

$$\mathrm{DC}_j = \frac{\sum_{i=1}^{N-1} \boldsymbol{A}_{ij}}{N-1}, \quad (8)$$

$$\mathrm{SD}_j = \frac{\sum_{i=1}^{N-1} Q_{ij}\boldsymbol{A}_{ij}^{Q} d_{ij}}{\sum_{i=1}^{N-1} Q_{ij}\boldsymbol{A}_{ij}^{Q}}, \quad (9)$$

$$\mathrm{CC}_j = \frac{2\beta}{k_j(k_j-1)}, \quad (10)$$

$$\mathrm{ND}_j = k_{\mathrm{in}} - k_{\mathrm{out}}, \quad (11)$$

where N is the total number of vertex of grid point present in the complex network. d_{ij} denotes the distance between grid points i and j. k_j represents the number of grid points that are connected to grid point j, the maximum number of possible connections between these grid points are $k_j(k_j-1)/2$, whereas the number of actual connections present in the complex network is β. Additionally, k_{in} refers to the number of incoming connections while k_{out} indicates the number of outgoing connections.

3. Results and discussion

3.1. Statistical characteristics of heatwaves over China in the past 63 years

Based on the definition of heatwaves mentioned above, heatwave events at various grid points across China are assessed, and relevant characteristic indicators, including frequency, duration, earliest onset date, and latest end date, are calculated.

Figure 1 illustrates the temporal trends of heatwave frequency, total duration, and their corresponding standard deviations. The results show a significant increasing trend in both average heatwave frequency and total duration from 1961 to 2023. Specifically, heatwave frequency approximately rises from 3 occurrences to 5, while total duration increases from 15 days to about 30 days, nearly doubling. This trend is closely linked to global climate warming; as global temperatures increase, both the frequency and intensity of extreme weather

events likes heatwaves, are also rising. Although the changes in standard deviation are not significant, there is a slight increase, indicating a minor rise in the volatility of heatwave occurrences. This suggests that, despite the overall increase in the number and duration of heatwaves, the variability between different years has also intensified, with certain years experiencing a marked increase in heatwaves while others see relatively fewer occurrences.

Next, figure 2 illustrates the spatial distribution of heatwave frequency, total duration, average duration, and maximum duration of a single event from 1961 to 2023. The results reveal that Xinjiang, the middle and lower Yangtze River, and eastern China are key regions where heatwaves are both frequent and intense. For individual event, a distinct latitudinal gradient is observed: mid- and low-latitude regions experience longer average and maximum durations compared to high-latitude regions, indicating more severe heatwaves. Notably, the highest values of maximum duration for single events are concentrated in the Sichuan and Chongqing, highlighting the extremity of heatwaves in these areas, consistent with recent records of extreme heatwaves. Additionally, normality tests on heatwave occurrence frequency and total duration, using histograms and Q–Q plots, indicate that both indicators follow a normal distribution. This suggests a statistically symmetric distribution, with few extreme values and most data points clustered around the mean. These distributional characteristics reflect the stability of heatwave events and align with a recent study[45] showing that the rate of heatwave warming at global and hemispheric scales matches the global median, with no evidence of accelerated warming trends.

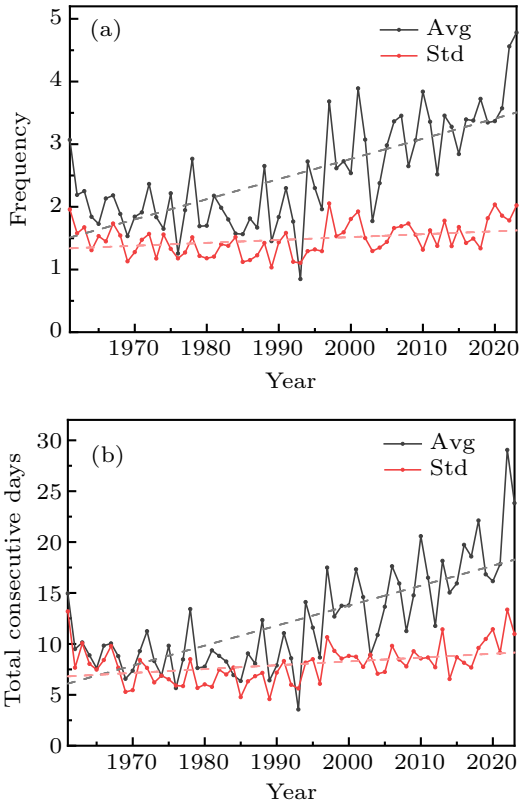


Fig. 1. The average (Avg) and standard (Std) deviations of (a) heatwave frequency, (b) total duration of heatwaves from 1961 to 2023.

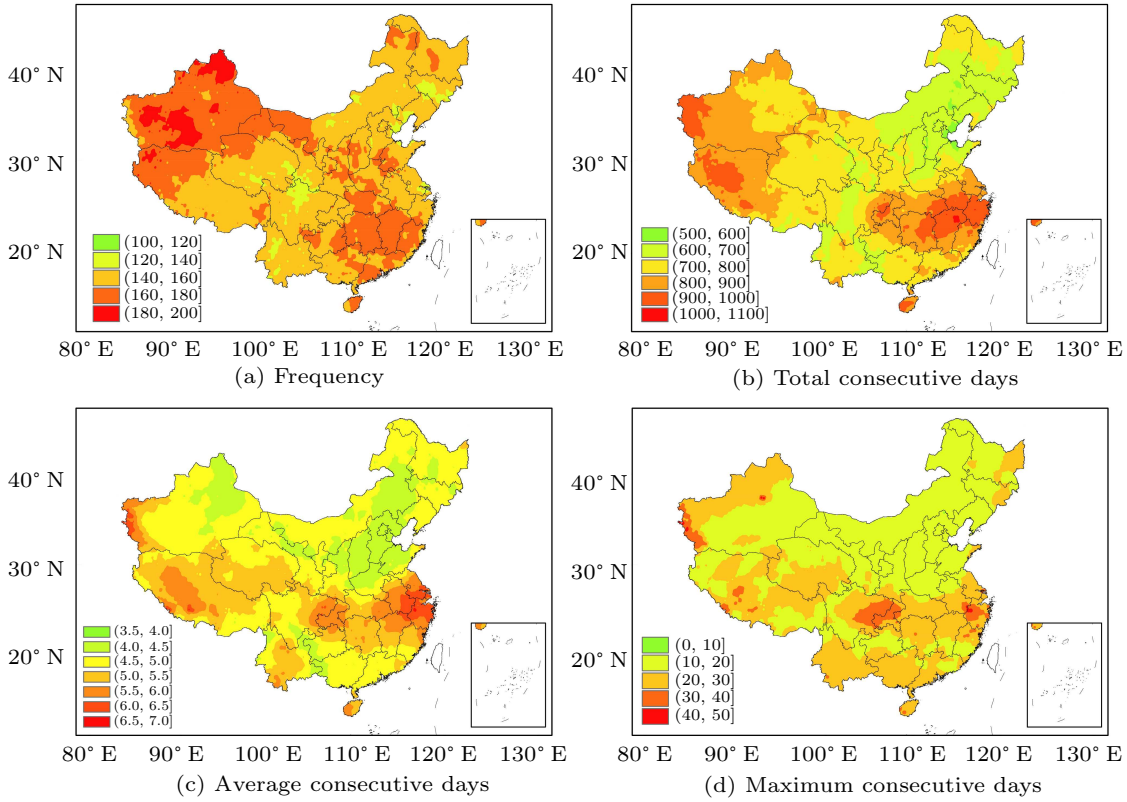


Fig. 2. (a) Frequency, (b) total consecutive days, (c) average consecutive days, and (d) maximum consecutive day of a single event at each grid point from 1961 to 2023.

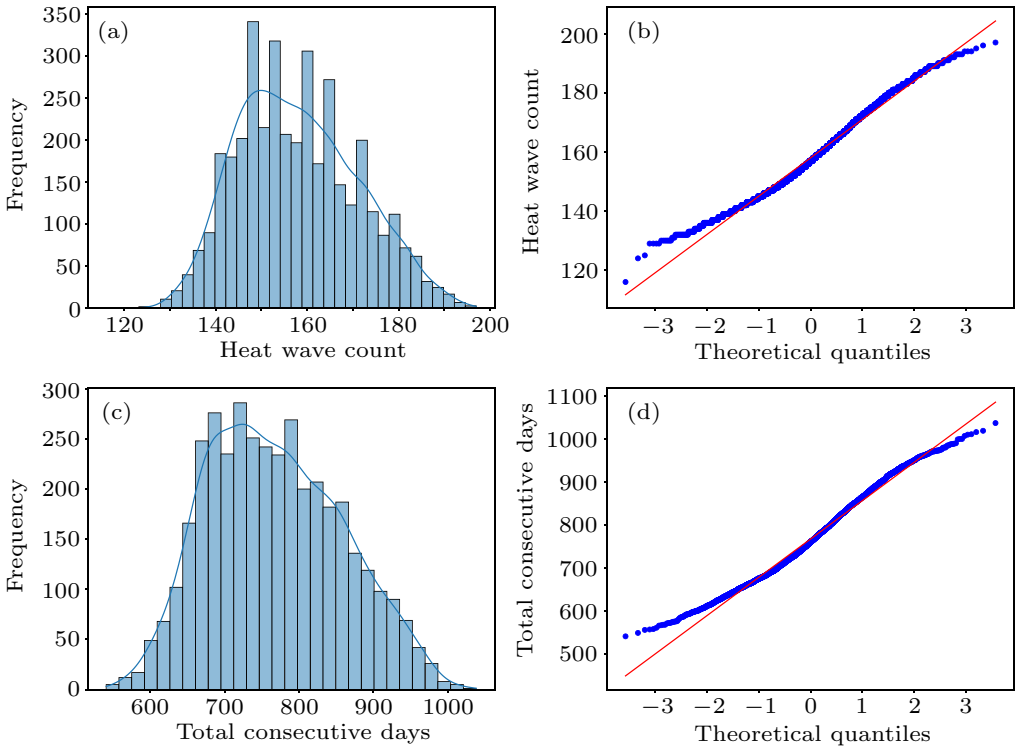


Fig. 3. Histogram and Q–Q plot of heatwave frequency and total duration.

After compiling heatwave data for each grid point, figure 4 illustrates the distribution of the earliest onset and latest end dates of heatwaves. It is worth noting that an unusual phenomenon is observed in 1974, where the frequency of heatwaves occurring in October is abnormally high. This is due to the normalized data represents the relative frequency variation of different months. The high frequency in October 1974 indicates that the number of heatwaves in that month was greater than in other years. This normalization eliminates inter-annual differences in total occurrences, allowing for a clearer comparison of relative changes between months across years, rather than focusing on absolute frequencies, which makes the data fairer and more intuitive when comparing across years.

The results reveal that heatwaves typically first emerge in July, with their onset progressively shifting earlier into June since the 2000s. The latest end dates have frequently occurred in August, particularly after the 2000s. Notably, since 2010, there has been an increasing likelihood of heatwaves beginning as early as May and extending into September or even October. This trend indicates a more pronounced "early onset and late retreat" pattern for heatwaves, signifying a yearly rise in both intensity and duration, along with the potential for more frequent and prolonged high-temperature events in the future. Despite the overall analysis revealing the evolutionary trends across China, the vast geographical expanse and significant differences in climatic characteristics, geographical conditions, and socio-economic backgrounds make it challenging for a single, unified analysis to fully capture regional variations. Therefore, further regional studies are necessary to better characterize the evolution of heatwaves in different areas. Based on this, China is divided into eastern and western regions along the 100°-E longitude, a critical boundary separating the monsoon and non-monsoon zones. This classification facilitates a clearer identification of temporal variations across different regions and provides a stronger basis for developing targeted early-warming and adaption strategies for climate change.

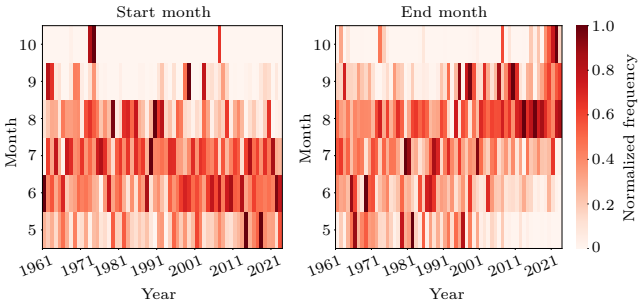


Fig. 4. Distribution of the earliest occurrence date and the latest disappearance date of heatwaves over China.

The results show that July is the peak month for the initial occurrence of heatwaves in both regions. However, since the 2000s, the eastern region has seen a higher frequency of heatwaves beginning in June compared to the western region. In the western region, heatwave retreat remains stable, mainly occurring in August. Conversely, the eastern region exhibits a more depressed pattern, spanning July, August, and September. This indicates that the East Asian summer monsoon sig-

nificantly influences heatwave dynamics in China, with earlier onset in the east. Additionally, variations in the monsoon system lead to greater fluctuations in heatwave occurrence and retreat timings in monsoon-affected areas.

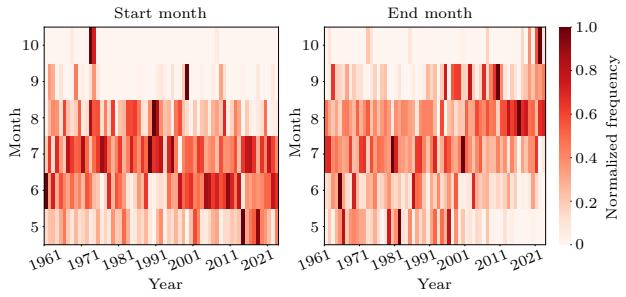


Fig. 5. Distribution of the earliest occurrence date and the latest disappearance date of heatwaves over east of 100° E in China.

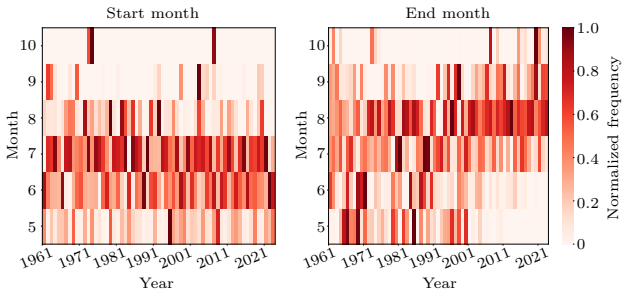


Fig. 6. Distribution of the earliest occurrence date and the latest disappearance date of heatwaves over west of 100° E in China.

3.2. Spatiotemporal evolution characteristics of heatwaves based on the event synchronization theory

3.2.1. Construction of complex network of heatwaves over the past 63 years

Utilizing the event synchronization method, undirected and directed networks of heatwave occurrences in China over the past 63 years have been established, alongside the computation of relevant network coefficients. In the realm of complex network science, degree centrality quantifies the number of nodes that synchronize with a given node, thereby indicating the node's connectivity strength within the network. In this analysis, the degree centrality of grid points signifies the quantity of neighboring points where heatwaves coincide within the defined maximum time lag. Prior studies have demonstrated that nodes with high degree centrality often function as "hubs" or "super nodes," which are critical to the integrity of the entire network structure. Moreover, synchronization distance serves as a measure of the temporal correlation between heatwave occurrences across various regions; greater synchronization distances suggest that heatwave events in those areas occur asynchronously relative to others. Notably, the distribution of synchronization distances exhibits a correlation with degree centrality (see Fig. 7(d)).

Figures 7(a) and 7(b) indicate that Xinjiang, parts of Northeast China (primarily western Heilongjiang and the border between Heilongjiang and Inner Mongolia), as well as the middle and lower reaches of the Yangtze River, exhibit both high degree centrality and synchronization distances. This suggests that these regions serve as critical nodes for heatwave propagation due to their strong connections with other areas. At the same time, the high synchronization distance reflects that heatwave events in these regions can influence broader spatial scales, making them core areas for heatwave transmission. In contrast, the southeastern coastal areas display lower degree centrality and shorter synchronization distances, indicating that heatwaves here are more localized with a smaller impact ranges and occur in closer alignment with surrounding areas.

Xinjiang represents a typical continental climate zone characterized by frequent extreme high temperatures. During summer, intense solar radiation leads to rapid surface warming; however, the low humidity hampers heat dissipation through evaporation, resulting in more frequent and intense heatwaves. Furthermore, the region's complex topography exacerbates this situation. The elevation differences between the northern and southern Tianshan Mountains, along with the basin structures such as the Tarim Basin, facilitate heat accumulation within the basins and impede its dispersal, creating persistent heat centers. Additionally, Xinjiang is situated in the westerly wind belt, where the influence of warm ridges during summer further amplifies heatwave occurrences and strengthens its connections with regions at similar latitudes.

The middle and lower reaches of the Yangtze River constitute another region highly susceptible to heatwaves, likely linked to the dynamics of the Western Pacific Subtropical High. When this system intensifies and extends westward, the area frequently experiences prolonged periods of hot weather with sustained high temperatures. The flat terrain hinders the dispersal of moist air, making it difficult to alleviate localized high temperatures, thereby facilitating the persistence of heatwaves. Located at the northern edge of the East Asian summer monsoon, these monsoon oscillations strengthen the correlation between climatic events in this region and those in surrounding areas.

The study also reveals the existence of a heatwave center in Northeast China, specifically in the western part of Heilongjiang Province and along the border with Inner Mongolia, an aspect that has received limited attention in previous research. Although summer temperatures in this region are relatively low, the Greater Khingan Range blocks cold air from the northwest, resulting in localized temperature increases. Additionally, the descending airflow associated with the mountains often leads to a "foehn effect," further elevating local temperatures. As a crucial node in atmospheric circulation, fluctuations in the westerly jet stream and monsoon systems can transmit heatwave characteristics from other regions to this area, establishing strong connections with heatwaves occurring elsewhere in the network.

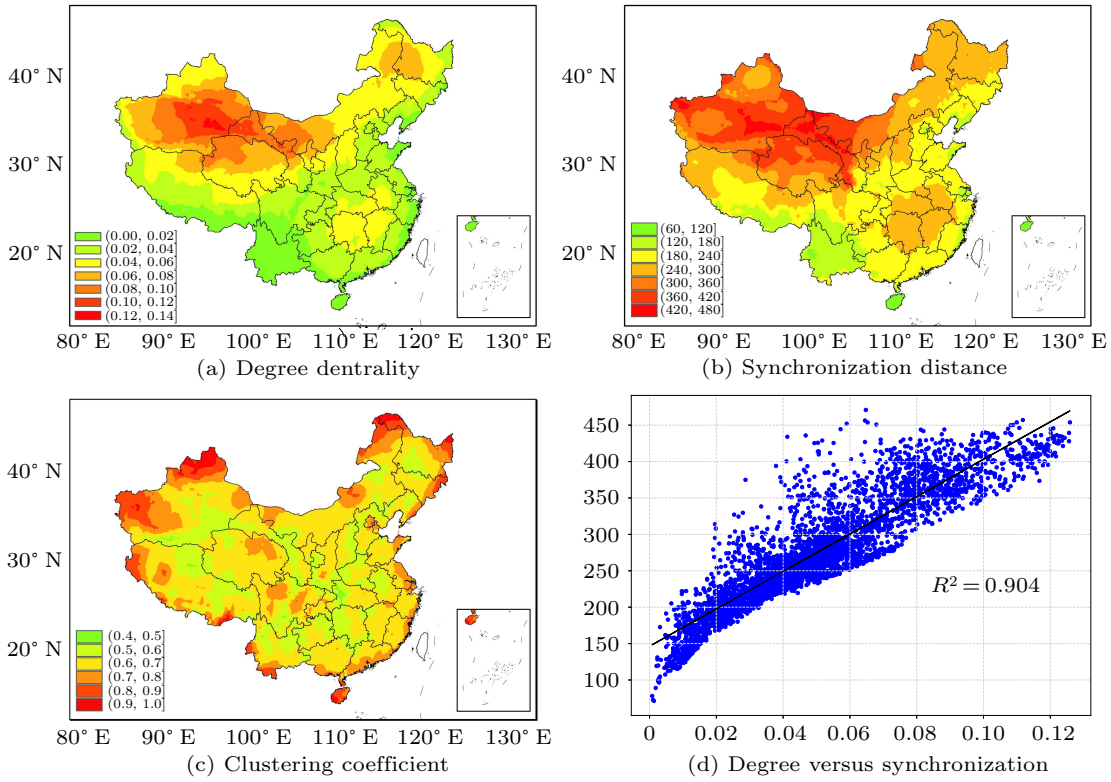


Fig. 7. (a) Degree centrality, (b) synchronization distance, (c) clustering coefficient, and (d) spatial correlation of degree centrality and synchronization distance based on undirected networks.

In contrast, the southeastern coastal regions exhibit lower degree centrality, primarily due to the moderating influence of the East Asian summer monsoon. The summer monsoon brings moist air and precipitation from the ocean, suppressing high temperatures and preventing heatwave propagation inland. Additionally, typhoons and tropical cyclones can disrupt prolonged heatwaves, reducing heat accumulation. Consequently, heatwaves here have a more localized impact, with relatively stable temperature variations, and are more synchronized with surrounding regions, reflected by a shorter synchronization distance.

In summary, the heatwave centers in Xinjiang, parts of Northeast China, and the middle and lower reaches of the Yangtze River are the result of multiple climatic mechanisms, including atmospheric circulation, monsoon systems, subtropical high pressure, and topography. The higher degree centrality of these regions underscores their critical role in the propagation of heatwave events across the country, while the large synchronization distances reflect the broader spatial influence and temporal differences of heatwave occurrences in these areas.

The clustering coefficient indicates the degree of connectivity among regions in the network. A high clustering coefficient indicates that heatwave synchronization at a given grid point is not only related to its surrounding grid points but also that these surrounding grid points exhibit strong synchronization with one another, forming a local heatwave synchronization cluster. High values are found in northern China (especially northern Xinjiang), the southwest, and the southeastern coast, suggesting that these areas form tighter networks with neighboring regions, making extreme events more likely to cluster locally. High degree centrality and high clustering coefficients can coexist: high centrality indicates broad connections to other areas, while high clustering reflects tight local clusters. For instance, Xinjiang and the northwestern regions exhibit strong external connections alongside close-knit internal networks.

Based on the directed network analysis, k_{in}, k_{out}, and the network divergence has been calculated. k_{in} refers to the number of heatwave events received by a grid point from others, while k_{out} refers to the number of heatwave events sent from a grid point to others. A high positive divergence indicates that the number of incoming connections to a grid point exceeds the number of outgoing connections, designating the area as a "sink." Conversely, a high negative divergence signifies that outgoing connections surpass incoming ones, classifying the area as a "source." As seen in Fig. 8, the highest negative value is observed in Xinjiang, corresponding to its high degree centrality, highlighting the region's significant role as a "source" in the national heatwave network. According to Fig. 7(c), Xinjiang's "source" function is evident as it transmits heat to neighboring areas. This is consistent with the conclusions of some researchers,[46–48] who have pointed out that the propagation of heatwaves in Xinjiang is influenced by regional zonal circulation and complex topography. As a result, heat is mostly confined to Xinjiang and its neighboring

regions, with limited extension to distant areas. High positive divergence is noted in the central inland regions, likely influenced by incoming heat from surrounding areas, which is consistent with findings from some studies, suggesting that the subtropical high and westerlies play a crucial role in directing heatwave events into inland regions, particularly during summer when these systems are most active.[49–51] This mechanism, coupled with feedback effects such as the stagnation and amplification of heatwaves, underscores the critical role of the central inland region as a "sink" in the heatwave propagation network.

However, regions previously identified as heatwave centers, such as the Heilongjiang–Inner Mongolia border and the middle and lower Yangtze River, show minimal divergence values. This may stem from complex local climate systems that both generate their own heatwaves and absorb external influences, though frequent fluctuations prevent clear "source" or "sink" roles. At the Heilongjiang–Inner Mongolia border, the Greater Khingan Range blocks northwest cold air, and local foehn effects amplify heat, but these impacts are largely localized with limited heat transfer, resulting in minimal divergence. In the middle and lower Yangtze region, while heatwaves are frequent, flat terrain and humid air create a stable climate. Active monsoon periods bring rain that moderates temperatures, limiting heatwave duration and reach. In summary, these regions likely act as self-contained heatwave centers rather than relying on external heat transfer, functioning more as independent heatwave hubs than as significant "sources" or "sinks" in the network.

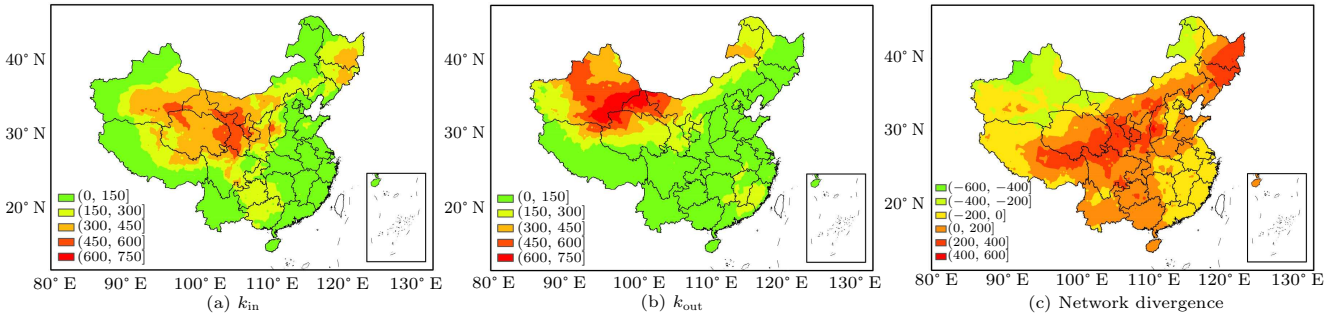


Fig. 8. (a) k_{in}, (b) k_{out}, and (c) network divergence based on directed networks.

3.2.2. Construction of complex network of heatwaves in different time periods

The results in Fig. 1 indicate that 1993 represents the lowest point in both average heatwave frequency and total duration across grid points. Previous studies have similarly identified 1993 as a key change point through mutation detection tests.[52] As a result, the 63-year period has been divided into two intervals, 1961–1993 and 1994–2023, to build complex networks based on event synchronization, facilitating a comparative analysis of heatwave patterns between these timeframes. This division not only reveals the spatial distribution characteristics of heatwave events across different periods but also identifies the changes in complex network features within the region. Moreover, this division aligns with the accelerated global warming background, providing a more precise analytical framework for studying the spatiotemporal evolution of heatwave events in China and their climatic driving mechanisms.

In both periods, Xinjiang consistently emerges as a region of high-degree centrality, underscoring its central role in the heatwave network structure across both intervals. Parts of Northeast China and the middle and lower Yangtze River regions also display elevated degree centrality, indicating strong connectivity within the network. As in previous findings, synchronization distance and degree centrality are strongly positively correlated for each period. From 1994 to 2023, the extent of low degree centrality and synchronization distances decreased, indicating an expanded influence and stronger spatiotemporal connectivity of heatwaves compared to 1961–1993. This trend likely stems from the intensified frequency, spread, and propagation of heatwaves associated with global warming. Additionally, clustering coefficients have risen across most regions since 1994, with substantial increases in the southeastern coastal areas and the Sichuan Basin, suggesting stronger local connectivity and heightened synchronization of heatwave events within these areas.

In summary, from 1994 to 2023, heatwaves demonstrate stronger network centrality and an expanded spatial influence. These changes underscore the intensifying influence of global warming on heatwave characteristics, emphasizing the need for increased attention and adaptive measures to address these evolving climate risks.

Figure 11 presents the network divergence distribution across two periods based on directed network analysis. Xinjiang consistently emerges as a divergence region in both periods, though its divergence has weakened from 1994 to 2023. While Xinjiang remains a source region, its influence on other areas has lessened, likely due to its relatively enclosed topography and the northward shift of zonal circulation during the warm season. This combination restricts the spread of heat-

waves mostly to Xinjiang and nearby northern regions, limiting the effective transfer of heat to eastern and southern China. However, the extent of high positive values in Central China has decreased from 1994 to 2023. This change may not only be attributed to local climate characteristics but also reflect the influence of more complex global climate mechanisms. Specifically, global warming has triggered multiple systemic changes, such as the northward migration of the subtropical

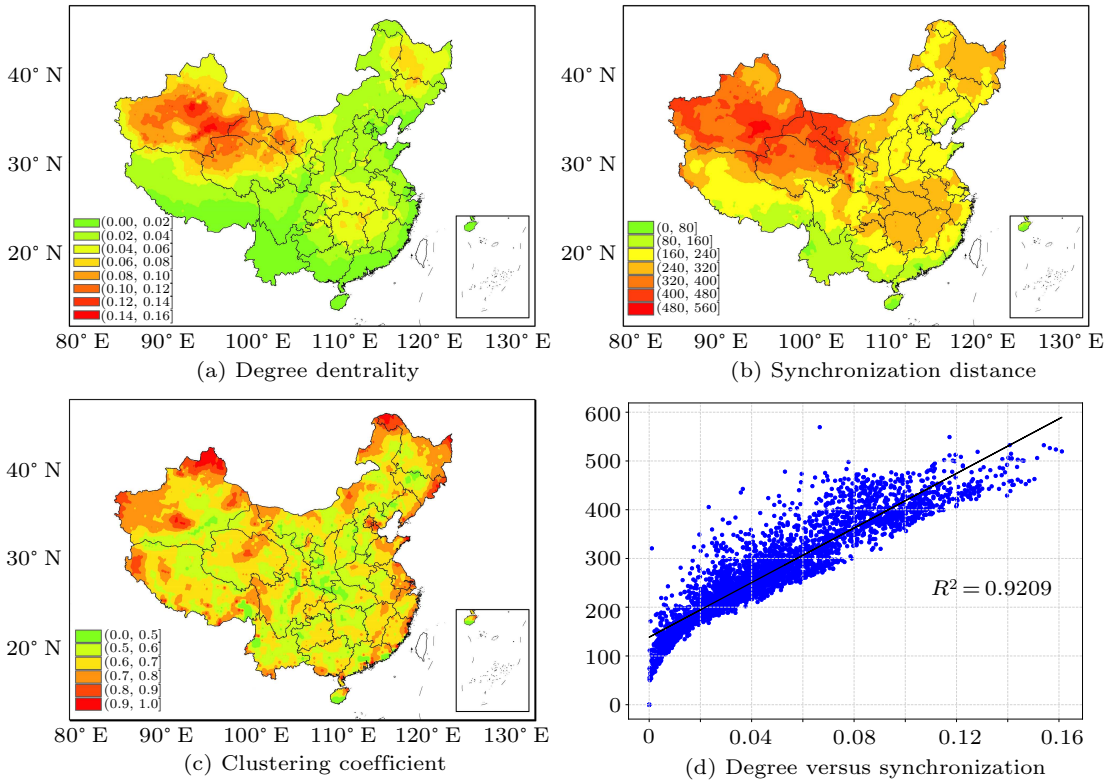


Fig. 9. (a) Degree centrality, (b) synchronization distance, (c) clustering coefficient, (d) spatial correlation between degree centrality and synchronization distance based on the undirected network from 1961 to 1993.

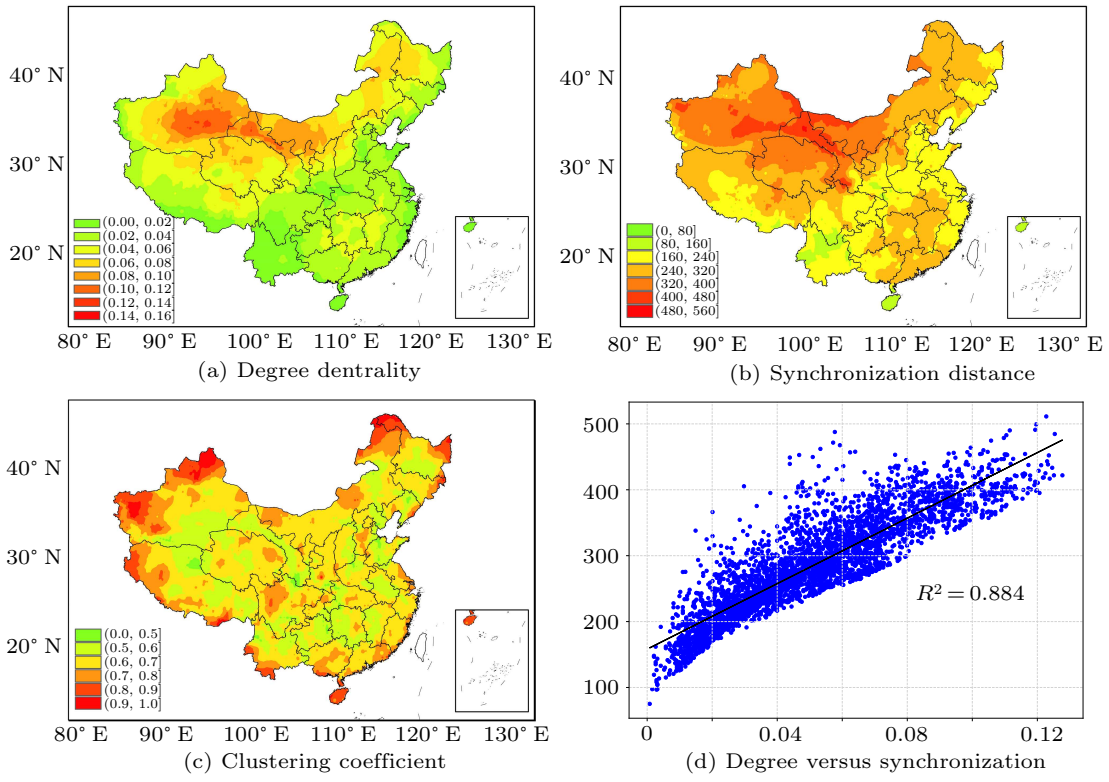


Fig. 10. (a) Degree centrality, (b) synchronization distance, (c) clustering coefficient, (d) spatial correlation between degree centrality and synchronization distance based on the undirected network from 1994 to 2023.

high, weakening of the polar vortex, and fluctuations in the westerlies, which may have reshaped the pathways of heatwave propagation. For example, adjustments in monsoon pathways might have reduced external heat inputs to Central China, while the region's flat terrain and stalling effects likely enhanced the persistence of local heatwave events. Additionally, feedback mechanisms within the climate system, such as land-atmosphere coupling and soil moisture deficits, may have amplified the local characteristics of heatwaves in Central China while reducing the efficiency of external heat transfer. These shifts underscore the significant effect of global warming on the spatiotemporal distribution of heatwaves in China, while highlighting the regulatory roles of regional climate systems, such as the subtropical high and local atmospheric circulation, in shaping heatwave propagation dynamics over China.

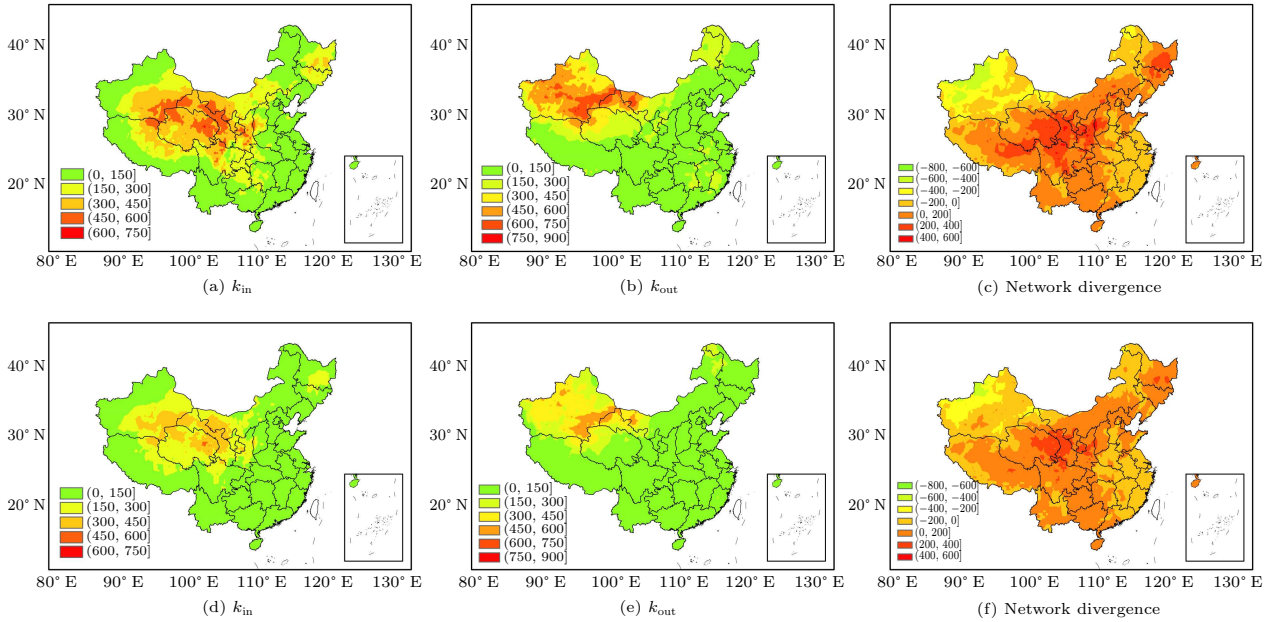


Fig. 11. The k_{in}, k_{out}, and network divergence of the directed network from 1961–1993 [panels (a)–(c)] and 1994–2023 [panels (d)–(f)].

4. Conclusion and perspectives

This study primarily employs the event synchronization method within a complex network framework, in combination with traditional statistical methods, to systematically analyze heatwaves in China from 1961 to 2023. By constructing undirected and directed heatwave networks, the study explores the spatiotemporal characteristics of heatwave events across various regions.

The analysis reveals a marked increase in heatwaves over China, with both the frequency and duration nearly doubling. This trend is especially pronounced in the middle and lower Yangtze River basin and Xinjiang, now established as high-frequency heatwave regions. Additionally, heatwaves in China display a more distinct pattern of "early onset and late retreat," reflecting an annual rise in both intensity and duration, which suggests more frequent and prolonged high-temperature events may lie ahead. The East Asian summer monsoon strongly influences heatwave timing, with eastern regions experiencing earlier heatwaves compared to western areas. Monsoon fluctuations also create greater variability in the timing of heatwave onset and retreat within these regions. Complex network analysis further reveals the dynamic behavior of heatwaves: metrics such as degree centrality and synchronization distance highlight the middle and lower Yangtze River basin, Xinjiang, and Northeast China as pivotal nodes in heatwave propagation. Between 1994 and 2023, heatwave events in China demonstrate stronger network centrality and more complex synchronization patterns.

The findings from both analytical approaches are complementary: traditional statistical methods reveal overall trends in heatwaves, while complex network analysis captures their finer spatiotemporal dynamics. Nonetheless, this study has some limitations. First, the maximum time lag for heatwave propagation was set at three days; future research could consider longer time lags to identify additional heat source and sink regions, potentially uncovering the effects of multi-scale time lags on heatwave behavior. Second, while the meteorological data used here provide broad coverage, the limited spatial resolution may miss certain localized climate phenomena. Data with higher resolution could enhance the detection of small-scale heatwave events. Finally, given the strong link between heatwave occurrences and atmospheric circulation systems in China, further research could explore the connections between surface heatwaves and circulation factors (such as geopotential height and wind speed) and work toward identifying early warning signals.

Acknowledgements

Project supported by the National Key Research and Development Program of China (Grant Nos. 2022YFE0136000 and 2024YFC3013100), the Joint Meteorological Fund (Grant No. U2342211), and the Joint Research Project for Meteorological Capacity Improvement (Grant No. 22NLTSZ004) and the National Meteorological Information Center (Grant No. NMICJY202301).

References

[1] Muri H, Tjiputra J, Otterå O H, Adakudlu M, Lauvset S K, Grini A, Schulz M, Niemeier U and Kristjánsson J E 2018 *J. Clim.* **31** 6319
[2] Sun Y, Zhang X B, Zwiers F W, Song L C, Wan H, Hu T, Yin H and Ren G Y 2014 *Nat. Clim. Change* **4** 1082
[3] Lu C H, Shen Y C, Li Y H, Xiang B and Qin Y J 2022 *J. Meteorol. Res.* **36** 643
[4] Shi H B 2012 *Sci. Geogr. Sin.* **32** 866 (in Chinese)
[5] Ding T and Qian W H 2011 *Adv. Atmos. Sci.* **28** 322
[6] Zhai P M and Pan X H 2003 *Acta Geogr. Sin.* **58** 1 (in Chinese)
[7] Lin X and Guan Z Y 2008 *Trans. Atmos. Sci.* **31** 1 (in Chinese)
[8] Sun J Q, Wang H J and Yuan W 2011 *Clim. Environ. Res.* **16** 199 (in Chinese)
[9] Dong X Y and Wu B Y 2019 *J. Appl. Meteor. Sci.* **30** 431 (in Chinese)
[10] Li S S, Yang S N, Zhang D H and Liu X F 2015 *J. Appl. Meteor. Sci.* **26** 545 (in Chinese)
[11] Xie J H, Yu J H, Chen H S and Hsu P C 2020 *Adv. Atmos. Sci.* **37** 1435
[12] Zhang P, Dai E F, Wu C S and H J 2024 *Clim. Dyn.* **62** 841
[13] Yu E T and Sun J Q 2019 *Trans. Atmos. Sci.* **42** 46 (in Chinese)
[14] Qian W H and Lin X 2004 *Clim. Res.* **27** 119
[15] Yan Z, Jones P D, Davies T D, Moberg A, Bergström H, Camuffo D, Cocheo C, Maugeri M, Demarée G R, Verhoeve T, Thoen E, Barriendos M, Rodríguez R, Martín-Vide J and Yang C 2002 *Clim. Change* **53** 355
[16] Li J, Zhu Z W and Dong W J 2017 *Meteorol. Atmos. Phys.* **129** 273
[17] Zhang Z W and Shi X H 2010 *J. Qinghai Meteorol.* **4** 2 (in Chinese) CNKI:SUN:QHQX.0.2010-04-002
[18] Jia H and Yun S 2018 *J. Catastrophol.* **33** 223 (in Chinese)
[19] Horton R M, Mankin J S, Lesk C, Coffel E and Raymond C 2016 *Curr. Clim. Change Rep.* **2** 242
[20] Mondal S and Mishra A K 2021 *Geophys. Res. Lett.* **48** e2020GL090411
[21] An B K and Feng Y 2014 *Appl. Mech. Mater.* **651** 1811
[22] Wang Y and Wang J F 2021 *J. Forecast.* **40** 911
[23] Zhang P T, Ning P Y, Cao R H and Xu J W 2021 *Front. Phys.* **9** 702064
[24] Huang S, Chen J, Li M Y, Xu Y H and Hu M B 2024 *Chin. Phys. B* **33** 030205
[25] Hu X, Chen J X and Xia C Y 2024 *Chin. Phys. B* **33** 100202
[26] Boers N, Bookhagen B, Marwan N, Kurths J and Marengo J 2013 *Geophys. Res. Lett.* **40** 4386
[27] Konapala G and Mishra A 2017 *J. Hydrol.* **555** 600
[28] Malik N, Bookhagen B, Marwan N and Kurths J 2012 *Clim. Dyn.* **39** 971
[29] Mondal S, Mishra A K and Leung L R 2020 *Geophys. Res. Lett.* **47** e2020GL088185
[30] Feng A X, Gong Z Q, Wang Q G and Feng G L 2012 *Theor. Appl. Climatol.* **109** 635
[31] Feng A X, Wang Q G, Zhang S X, Enomoto T, Gong Z Q, Hu Y Y and Feng G L 2022 *Chin. Phys. B* **31** 049201
[32] Gong Z Q, Su H J, He S H and Feng G L 2017 *J. Trop. Meteorol.* **23** 426
[33] Gong Z Q, Zhou L, Zhi R and Feng G L 2008 *Acta Phys. Sin.* **57** 5351 (in Chinese)
[34] Hu H R, Gong Z Q, Wang J, Qiao P J, Liu L and Feng G L 2021 *Acta Phys. Sin.* **70** 249201 (in Chinese)
[35] He S H, Gong Z Q, Ye F and Feng G L 2017 *Acta Meteorol. Sin.* **75** 894 (in Chinese)
[36] Zhou L, Gong Z Q, Zhi R and Feng G L 2008 *Acta Phys. Sin.* **57** 7380 (in Chinese)
[37] Yang J H, Song J Q and Cao X Q 2013 *Acta Phys. Sin.* **62** 174102 (in Chinese)
[38] Hu J, Zhang Y J, Wu P and Li H J 2022 *Chaos, Solitons and Fractals* **154** 111613
[39] Ding T, Qian W H and Yan Z W 2010 *Int. J. Climatol.* **30** 1452
[40] Perkins-Kirkpatrick S E and Lewis S C 2020 *Nat. Commun.* **11** 3357
[41] Perkins S E 2015 *Atmos. Res.* **164–165** 242
[42] Alexander L V, Zhang X, Peterson T C, *et al*. 2006 *J. Geophys. Res. Atmos.* **111** D5
[43] Perkins S E, Alexander L V and Nairn J R 2012 *Geophys. Res. Lett.* **39** 1
[44] Quiroga R Q, Kreuz T and Grassberger P 2002 *Phys. Rev. E* **66** 041904
[45] McKinnon K A, Simpson I R and Williams A P 2024 *Proc. Nat. Acad. Sci. USA* **121** e2406143121
[46] Ning G C, Luo M, Zhang Q, Wang S G, Liu Z, Yang Y J, Wu S J and Zeng Z L 2021 *J. Geophys. Res. Atmos.* **126** e2020JD034111
[47] Kadier Z, Li Z Y, Abulikemu A, Zhu K F, Abulimiti A, An D W and Abuduaini A 2023 *Remote Sens.* **15** 4833
[48] Zhang X Y, Liu Y, Zhu Y, Ma Q, Philippe G, Qu Y P and Yin H 2023 *Hydrol. Res.* **54** 869
[49] Guo Y X and Fu Z T 2024 *Clim. Dyn.* **62** 665
[50] Chen X L and Zhou T J 2018 *Clim. Dyn.* **51** 4403
[51] Zhao R, Zhou X, Liu J, Li Y P, Huang G H and Li C H 2024 *J. Hydrol.* **639** 131635
[52] Wu J C, Zhu Y, Liu Y, Yin H, Yuan F and Wang J 2022 *J. China Hydrol.* **42** 72 (in Chinese)